



Solenoidal Micromagnetic Stimulation Enables Activation of Axons With Specific Orientation

Laleh Golestanirad^{1,2†}, John T. Gale^{3†}, Nauman F. Manzoor^{4,5}, Hyun-Joo Park⁴, Lyall Glait^{4,5}, Frederick Haer⁶, James A. Kaltenbach⁴ and Giorgio Bonmassar^{1,2*}

¹ Athinoula A. Martinos Center, Massachusetts General Hospital, Charlestown, MA, United States, ² Harvard Medical School, Boston, MA, United States, ³ Department of Neurosurgery, Emory University, Atlanta, GA, United States, ⁴ Department of Neurosciences, Cleveland Clinic Lerner Research Institute, Cleveland, OH, United States, ⁵ Ear, Nose and Throat Institute, University Hospitals Cleveland Medical Center, Case Western Reserve University, Cleveland, OH, United States, ⁶ Frederick Haer Corporation, Bowdoin, ME, United States

OPEN ACCESS

Edited by:

Christopher Basciano,
Becton Dickinson, United States

Reviewed by:

Yael Yaniv,
Technion – Israel Institute
of Technology, Israel
Arun V. Holden,
University of Leeds, United Kingdom

*Correspondence:

Giorgio Bonmassar
giorgio@nmr.mgh.harvard.edu

† These authors have contributed
equally to this work.

Specialty section:

This article was submitted to
Computational Physiology
and Medicine,
a section of the journal
Frontiers in Physiology

Received: 13 March 2018

Accepted: 24 May 2018

Published: 27 July 2018

Citation:

Golestanirad L, Gale JT, Manzoor NF,
Park H-J, Glait L, Haer F,
Kaltenbach JA and Bonmassar G
(2018) Solenoidal Micromagnetic
Stimulation Enables Activation
of Axons With Specific Orientation.
Front. Physiol. 9:724.
doi: 10.3389/fphys.2018.00724

Electrical stimulation of the central and peripheral nervous systems - such as deep brain stimulation, spinal cord stimulation, and epidural cortical stimulation are common therapeutic options increasingly used to treat a large variety of neurological and psychiatric conditions. Despite their remarkable success, there are limitations which if overcome, could enhance outcomes and potentially reduce common side-effects. Micromagnetic stimulation (μ MS) was introduced to address some of these limitations. One of the most remarkable properties is that μ MS is theoretically capable of activating neurons with specific axonal orientations. Here, we used computational electromagnetic models of the μ MS coils adjacent to neuronal tissue combined with axon cable models to investigate μ MS orientation-specific properties. We found a 20-fold reduction in the stimulation threshold of the preferred axonal orientation compared to the orthogonal direction. We also studied the directional specificity of μ MS coils by recording the responses evoked in the inferior colliculus of rodents when a pulsed magnetic stimulus was applied to the surface of the dorsal cochlear nucleus. The results confirmed that the neuronal responses were highly sensitive to changes in the μ MS coil orientation. Accordingly, our results suggest that μ MS has the potential of stimulating target nuclei in the brain without affecting the surrounding white matter tracts.

Keywords: eddy currents, TMS, finite element method, microcoils, inductive stimulation, numerical modeling, neurostimulation

INTRODUCTION

Implanted medical devices based on electrical stimulation such as cardioverter-defibrillators and pacemakers (Ellenbogen and Wood, 2008), spinal cord stimulation (Kreis and Fishman, 2009), and deep brain stimulation (DBS) (Montgomery, 2010) devices have become well-accepted therapeutic options to treat a wide variety of medical conditions. Electrical stimulation has considerable clinical impact in alleviating symptoms of an increasingly diverse range of neurological and psychiatric

disorders including for example, cochlear (Gifford, 2013) and auditory brainstem implants for restoring hearing (Møller, 2006), DBS to treat symptoms of Parkinsonism (Benabid, 2003; Deuschl et al., 2006), cortical stimulation for epilepsy and depression (Howland, 2008; Morace et al., 2016; Williams et al., 2016), spinal cord stimulation for neuropathic pain (Lopez et al., 2016), and vagus nerve stimulation for epilepsy (Panayiotopoulos, 2011) and depression (O'Reardon et al., 2006; United States Congress Senate Committee on Finance, 2006), just to mention a few. More recently, electrical stimulation has also shown promise for the restoration of function of retinal implants to restore vision in the blind (Humayun et al., 2012; Shepherd et al., 2013; Zrenner, 2013; Ayton et al., 2014; Stingl et al., 2015).

Although electrical techniques for neuronal stimulation have proven quite useful, they have several limitations that can be overcome by micro magnetic stimulation (μ MS) which uses sub-millimeter coils. For example, for an electrode pair to generate currents it needs to be placed in contact with a conductive media (e.g., excitable tissue). Electric currents that are delivered by these electrodes diffuse and can spread to undesired areas adjacent to the structures being targeted, leading to unintended side-effects (Histed et al., 2009; Behrend et al., 2011; Licari et al., 2011; Weitz et al., 2015). A magnetic coil, on the other hand, can induce electric currents in the tissue from a distance (i.e., through an insulation layer). In nature these currents are closed-loop circular currents with a higher spatial focality (Figure 1). Furthermore, the fact that μ MS coils can deliver stimulation while being insulated from the tissue increases their biocompatibility and compatibility with magnetic resonance imaging (considering no ferromagnetic material is present). Finally, as μ MS coils can be positioned within or immediately adjacent to the neural tissue, the power needed to evoke neuronal activities is significantly reduced compared to techniques such as transcranial magnetic stimulation (TMS) which are designed to generate strong magnetic fields that pass through the skull and deliver stimulation to the cortical tissue.

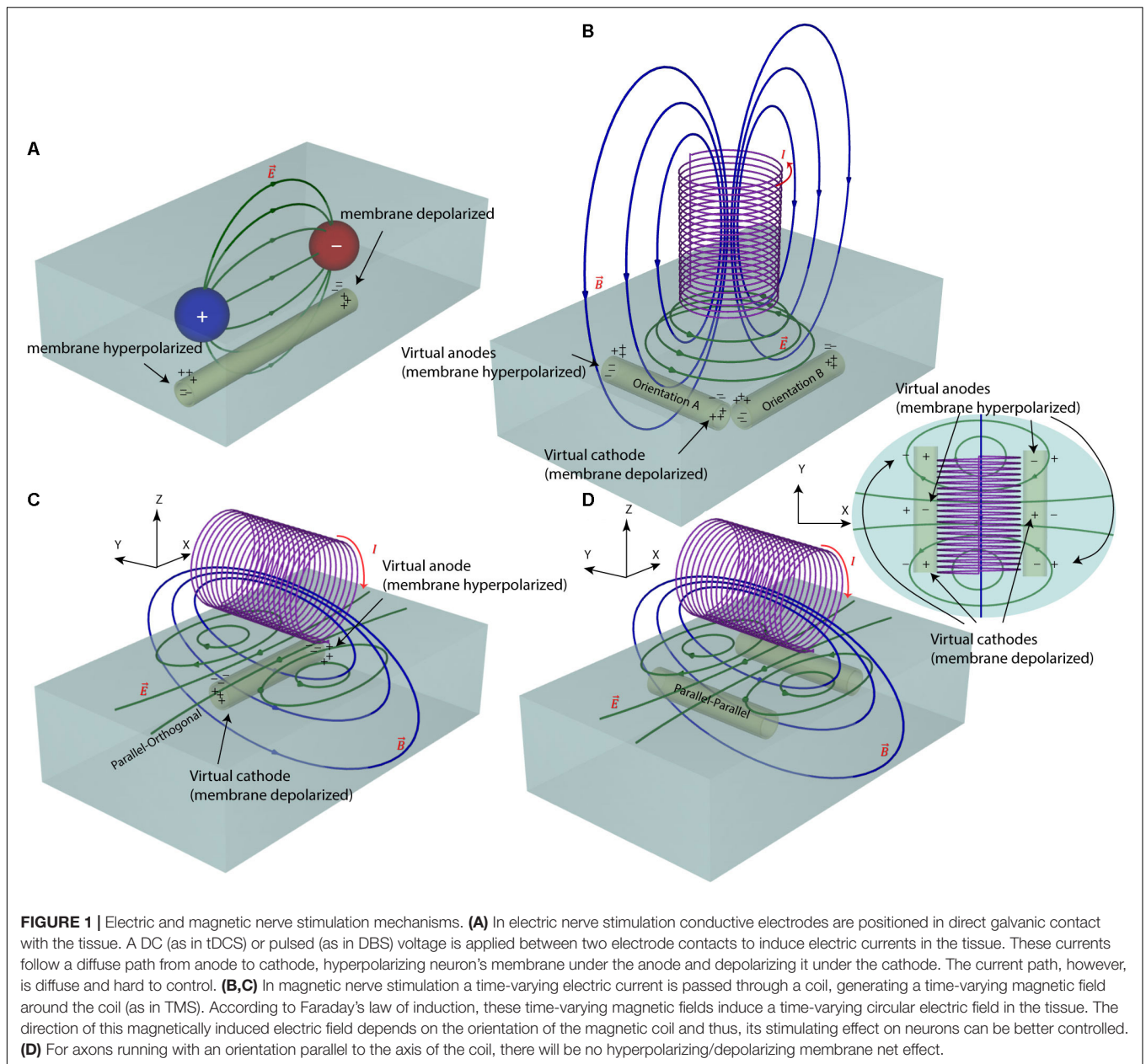
Our group recently demonstrated the feasibility of using μ MS to elicit neuronal activation *in vitro* (Bonmassar et al., 2012), as well as the activation of neuronal circuitry on the system level *in vivo* (Park et al., 2013). As μ MS is a novel technology, its mechanism(s) of nerve activation, induced field characteristics, and optimum topological features are yet to be explored. In this work, we performed numerical simulations to provide an insight into spatial distribution of μ MS-induced electric fields, which in turn dictate the dynamics of nerve stimulation threshold changes with different axonal directionalities. Electromagnetic simulations were performed to estimate the magnetic flux \vec{B} and the electric field \vec{E} and its spatial gradient at different distances from the coil. These simulations were based on the actual coil prototypes built (Figure 2) and utilized in our animal experiments (Figure 3). The estimated \vec{E} fields were then used in conjunction with the NEURON cable model to investigate the directional sensitivity of μ MS (Figures 4, 5). Finally, we performed *in vivo* experiments where we studied responses evoked in the inferior colliculus (IC) of rodents by applying μ MS stimuli to the

surface of animal's dorsal cochlear nucleus (DCN). Specifically, we examined the IC responses to different coil orientations (Figure 6).

METHODS

Electromagnetic Simulations

Numerical modeling has been long used to understand the phenomenology of field-tissue interaction in a wide variety of medical and diagnostic applications. Examples include use of electrostatic finite element modeling to predict the volume of activated tissue in electrical brain stimulation (McIntyre and Grill, 2001; Butson and McIntyre, 2006; Golestanirad et al., 2012b), eddy current modeling to assess the distribution of cortical currents in magnetic brain stimulation (Wagner T. et al., 2004; Wagner T.A. et al., 2004; Golestanirad et al., 2010, 2012c), and analysis of body exposure to low frequency magnetic fields and safety hazards due to motion of medical implants in magnetic fields (Condon and Hadley, 2000; Golestani-Rad et al., 2007; Golestanirad et al., 2012a). Recently, the role of numerical modeling has also been emphasized in safety assessment of MRI in patients with conductive implants (Clare McElcheran and Graham, 2014; Golestanirad et al., 2017a,b; McElcheran et al., 2017). The use of computational modeling to predict the response of neurons to external electric fields has been pioneered by eminent works of McIntyre and Grill (2001) and McIntyre et al. (2002, 2004) and followed by others (Wei and Grill, 2005; Wooock et al., 2010; Golestanirad et al., 2012b, 2013). Electromagnetic simulations have also been successfully applied to quantify induced currents and assess the safety of transcranial magnetic brain stimulation (Wagner T.A. et al., 2004; Golestanirad et al., 2010, 2012c; Deng et al., 2013). In this work, we used ANSYS Maxwell (ANSYS, Canonsburg, PA, United States) which solves a modified $T - \Omega$ formulation of Maxwell's Equations expressively designed for low-frequency calculations (Ren, 2002) using the finite element method (FEM). Simulations were performed with solenoidal μ MS coils (500 μ m diameter, 600 μ m height, 21 turns, wire diameter 7 μ m, carrying ~ 20 amperes for a total current per turn = 420 AT). Coils were placed 20 μ m above the surface of the tissue and were excited with a 70-kHz sinusoidal current. The tissue was modeled as a 10 mm \times 10 mm \times 1 mm slab of conductive material ($\sigma = 0.13$ S/m). The ensemble of the coil-tissue system was enclosed in a 14 mm \times 14 mm \times 6 mm air box with Neumann boundary conditions applied to its outer faces which ensured that magnetic field was tangential to the boundary and flux did not cross it. ANSYS Maxwell was set up to follow an adaptive mesh scheme. A high-resolution initial tetrahedral mesh (60 μ m) was seeded inside the tissue close to the coil. Maxwell generated a field solution using the specified mesh. It then analyzed the accuracy of the solution by calculating an energy value based on the error in the solution. The exact mechanism for evaluating the error varies by solution type. For eddy current solution, Maxwell uses $\nabla \times H$ to find current density and then subtracts all input currents and other sources. For a perfect solution, the result would be zero, whereas for a real finite mesh the

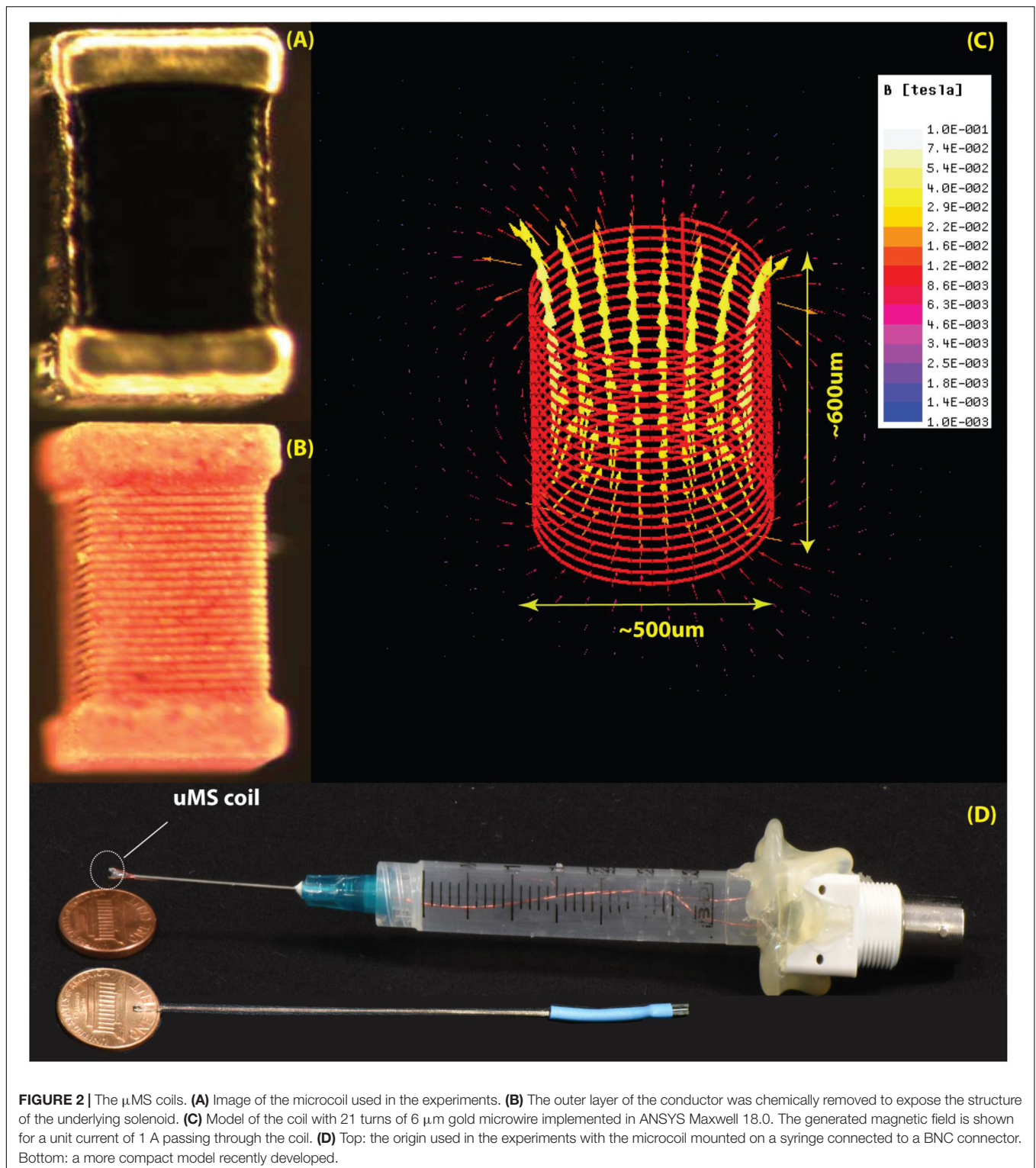


result would include some amount of residual current density. An energy value calculated from this residual current density is then used as the criteria to refine the mesh. An iterative process then will follow, which refines the mesh in each step until the energy error is below a user-specified value (1% in our case). The final solution had $\sim 630,000$ mesh elements with edge length varying from 9 μm inside the tissue to 2 mm at the outer boundary the air box. The simulations converged after two adaptive passes which completed in 17 h on a Dell PowerEdge R730 with 16x32GB = 512GB of RAM, an NVIDIA K80 GPU and 28 cores (2xIntel Xeon CPU with each 14 cores) running 64-bit Windows Server 2012. Electric field values were then exported to MATLAB (The Mathworks, Inc., Natick, MA, United States) for smoothing and were used to simulate

the response of neurons with different orientations below the coil.

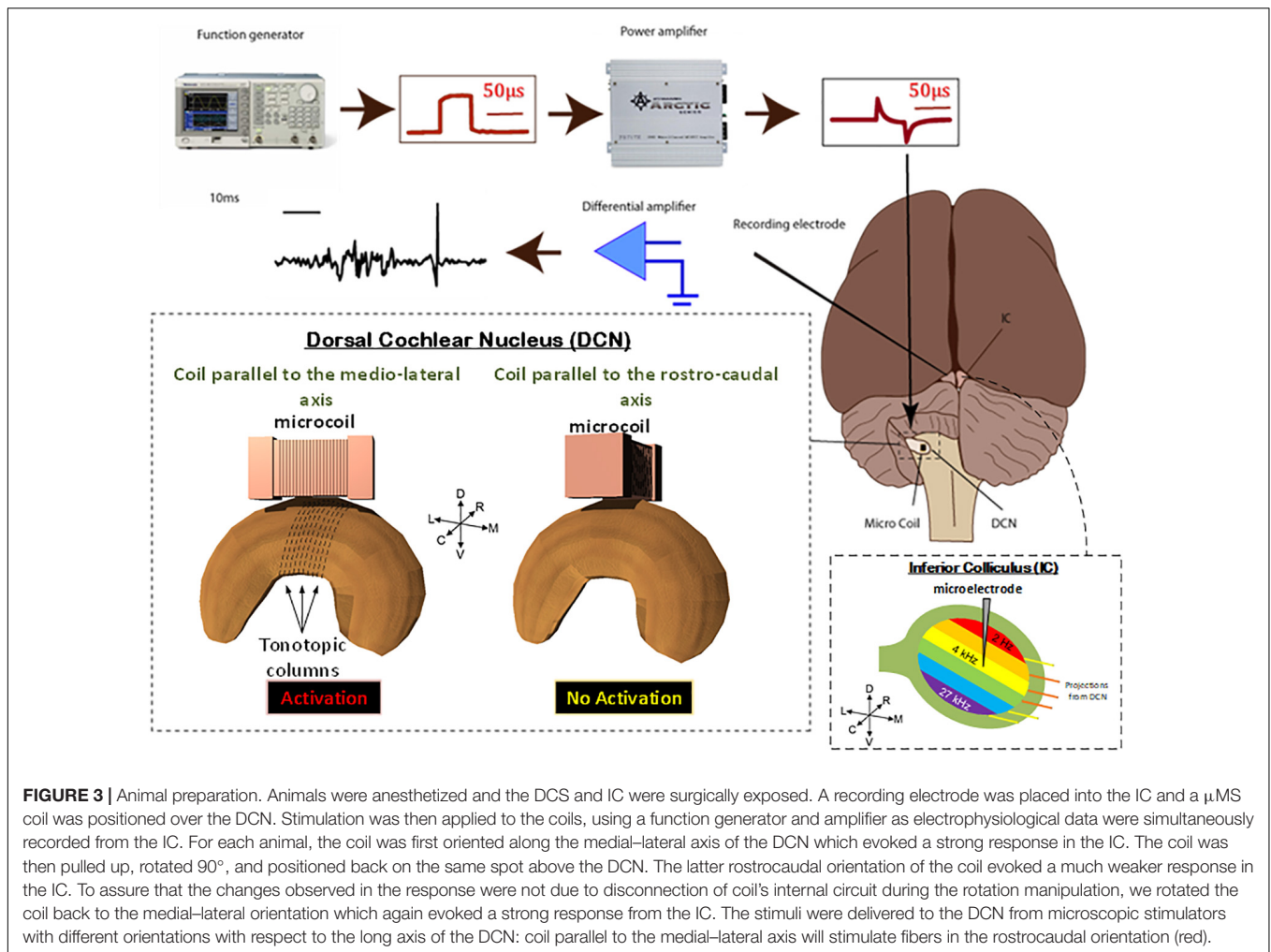
μ MS Coil Orientations

In our previous work (Bonmassar et al., 2012) we showed that response of ganglion cells to μ MS could be altered by changing the coil's orientation. Specifically, we demonstrated that when the long axis of a solenoidal μ MS coil was perpendicular to the surface of the excitable tissue (corresponding to **Figure 1B**), weaker neuronal responses were evoked compared to the case where the coil's long axis was parallel to the surface of the tissue. Our surgical setup at the time, however, did not allow further examination of μ MS directionality when the coil was parallel to the surface of the tissue. Theoretically, the



μ MS coil in a perpendicular orientation generates symmetric electric fields in the tissue underneath the coil, affecting axons with different orientations alike (see **Figure 1B**, axons with orthogonal orientations A and B experience similar electric field). This symmetry breaks down when the long

axis of the coil is parallel to the surface of the tissue. In theory, the parallel μ MS coil highly depolarizes axons that are located under its center and are orthogonal to its long axis (**Figure 1C**). We refer to this relative coil-axon orientation as the parallel-orthogonal orientation. In contrast,

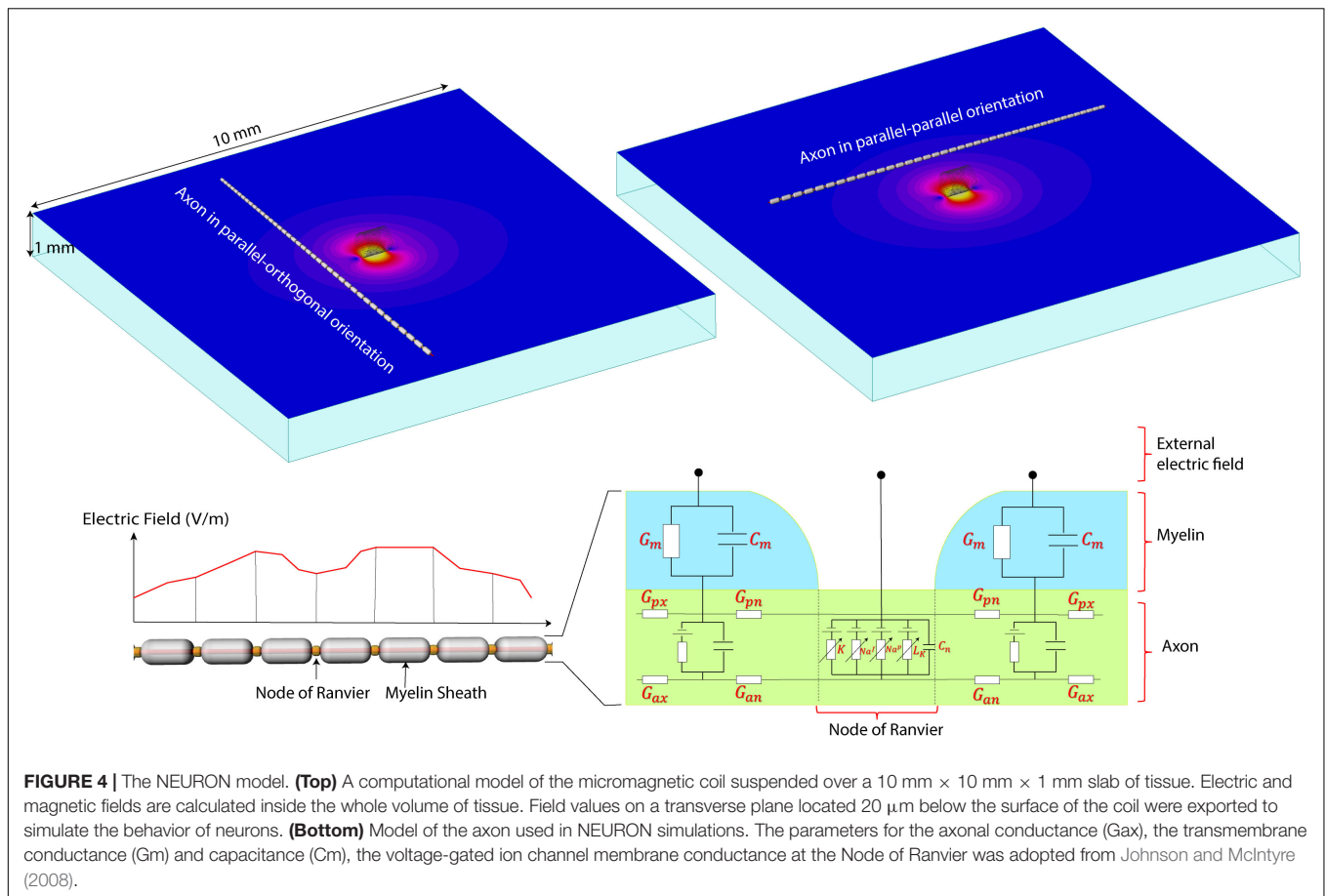


axons that are oriented parallel to the long axis of the coil (parallel-parallel orientation, **Figure 1D**) experience a reduced tangential electric field along with their length and should be minimally excited. We tested this hypothesis in NEURON simulations and in rodent experiments as described below.

Neuron Modeling

A computational model of axons was built for simulation of neuronal activation for the three-dimensional electric fields obtained in the previous section. The parallel fiber axon model was assumed to have a diameter of 2 μ m (Tolbert et al., 2004). Since the detailed information about the ion channels was not available, the ion channel properties were adopted from the double cable axon model of globus pallidus efferent axons (McIntyre et al., 2002; Johnson and McIntyre, 2008). In electrical or magnetic stimulation, the defining factor of axonal firing is the trans-membrane current at the nodes of Ranvier. When the transmembrane current is large enough to depolarize the membrane, an action potential initiates at the node and propagates both in the orthodromic and antidromic directions. Typically, the first node of activation is the node

closest to the cathode in electrical stimulation or the coil in magnetic stimulation. In our neuronal simulation, the outgoing transmembrane current was calculated by the summation of the axonal current from the adjacent compartments in the compartmental model (Nagarajan et al., 1993; McIntyre et al., 2002; Carnevale and Hines, 2006). The axonal directional current density in each compartment is calculated by the multiplication of the axonal conductivity and the induced electric field in the axonal direction. Since the compartmental size of the double cable axon model is so small, the induced electric field in each compartment was assumed to be constant. The axons were assumed to be in a transverse plane 20 μ m below the coil. The induced electric field at each compartment along the axon was obtained using bilinear interpolation of the electric field obtained in the previous section. A total of 41 axons were tested where the distance between each adjacent axon was set to 100 μ m. Each axon was assumed to have 41 nodes of Ranvier, and the intermodal distance was set to 200 μ m, and the center node was positioned at random distances from the coil. Regarding the orientation of the coil, we tested both the configurations where the axonal direction is parallel and orthogonal to the long axis of the coil. The software package NEURON was used to study the



neuronal responses to the induced electric fields (Carnevale and Hines, 2006).

Microcoil Construction

All microcoils were constructed to keep overall resistances below 5 Ω and inductances below 150 nH (4263B, Keysight Technologies, Santa Rosa, CA, United States) in order to ensure high stimulation efficacy. A multilayer inductor (ELJ-RFR10JFB, Panasonic Electronic Devices Corporation of America, Knoxville, TN, United States) was attached by soldering to two 34-AWG copper wires (Philmore Mfg., Rockford, IL, United States) with polyimide enamel inner coat and polyurethane overcoat. To insulate the tissue from the voltage applied and to protect against moisture, the microcoils were coated with an acrylic conformal coating (419C, MG = Chemicals, Burlington, ON, Canada) that offered high dielectric strength. The 419C Technical Data Sheet reports a thickness of 25 μ m with an estimated variability of the dielectric thickness to be $\pm 5 \mu$ m. After curing (24 h), the insulation of the microcoil was tested by immersing the coils in a saline solution (0.9% of NaCl) and verifying that the resistance between the microcoil and an EGG electrode also dipped in the saline solution was greater than 5 M Ω (TX3, Tektronix, Inc., Beaverton, OR, United States). The microscopic stimulator was placed on the tip of a 23 AWG needle (Becton Dickinson, Franklin Lakes, NJ, United States) and the two wires inserted in

the shaft/hub of the needle, and through the tip and barrel of a 3 ml syringe with the plunger that was removed and the flange end piece of the syringe was attached to a BNC connector by means of a glue gun, and electrically connected.

Magnetic Stimulation

Two adult male Syrian golden hamsters were studied in this work. All procedures performed were approved by the Institutional Animal Care and Use Committee of the Cleveland Clinic, which adheres to the NIH Guide for the Care and Use of Laboratory Animals. In each experiment, μ MS coils were mounted to a micromanipulator and manually positioned so that the coil was located just above the dorsal surface of the DCN, as described by Park et al. (2013). In our *in vivo* animal experiments, the μ MS coils were driven by a generator (AFG3021B, Tektronix, Inc., Beaverton, OR, United States) connected to a 1,000-W audio amplifier (PB717X, Pyramid, Inc., Brooklyn, NY, United States) with a frequency band up to 70 kHz. The output of the amplifier was connected to a BNC splitter so that the signal sent to the μ MS coil was monitored with an oscilloscope (DPO3012, Tektronix, Inc., Beaverton, OR, United States). Monophasic rectangular stimulation pulses with different pulse-widths and amplitudes were triggered by an analog A/D card (NI PCIe-6251, National Instruments), with an average rate of 2 Hz. The input pulse to the power amplifier and the corresponding output waveform of

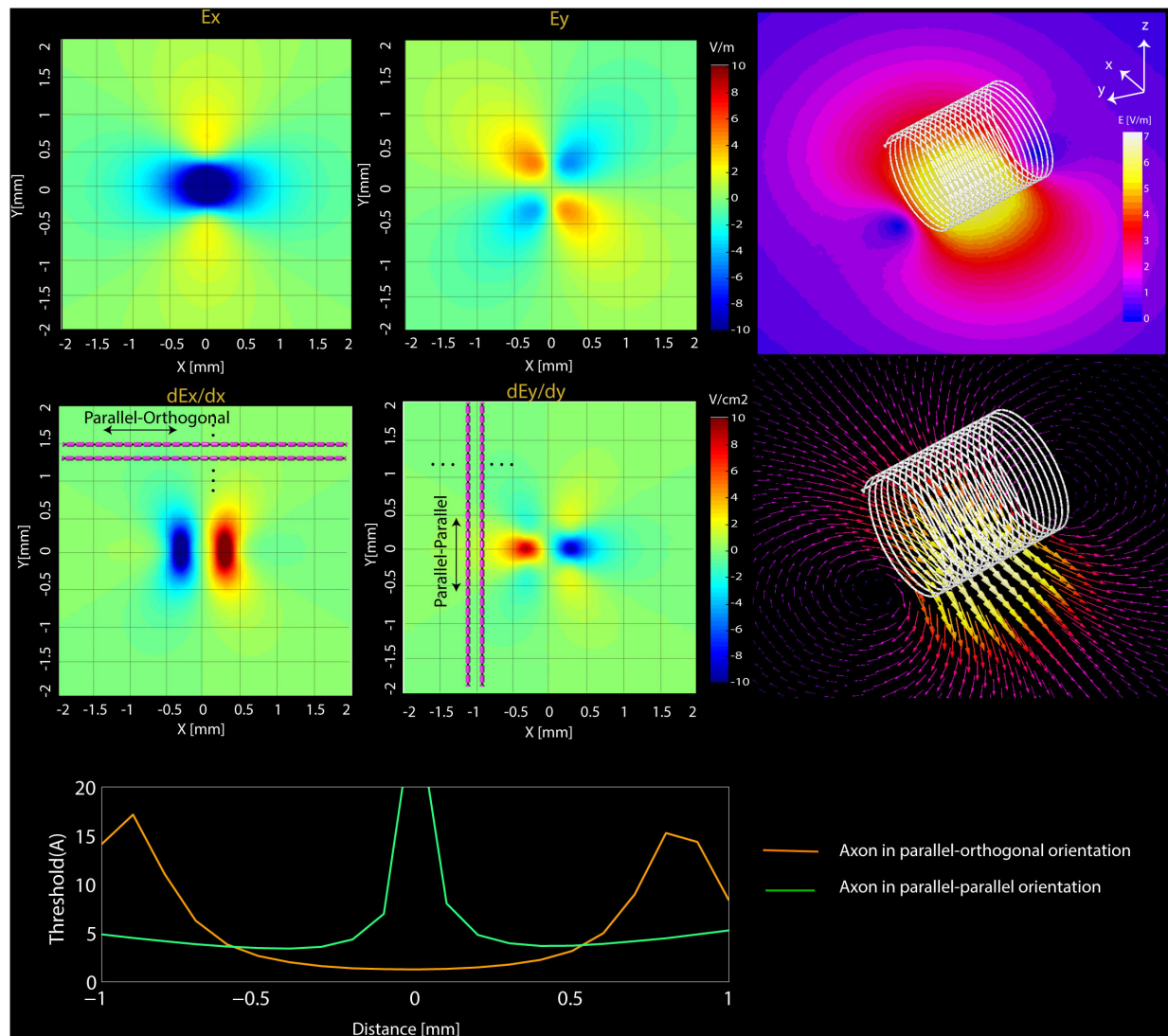


FIGURE 5 | Simulations results. **(Top)** Computational results of the magnitude of E_x and E_y and their spatial derivatives (dE_x/dx , dE_y/dy) on transverse planes located at $20\ \mu\text{m}$ below the surface of microcoil. **(Bottom)** NEURON estimated current threshold levels for the two orientations (orange-mediolateral and blue-rostrocaudal) at various distances from the axon.

the power amplifier are shown in **Figure 3**. When referencing ‘stimulus amplitude’ in this paper, we indicate only the input pulse amplitude to the power amplifier. To prevent the carrying over effect from the previous trial, the order of the stimulation parameters (pulse amplitude and pulse-width) was randomized for each animal in addition to allowing 30 s resting periods between each 60 s.

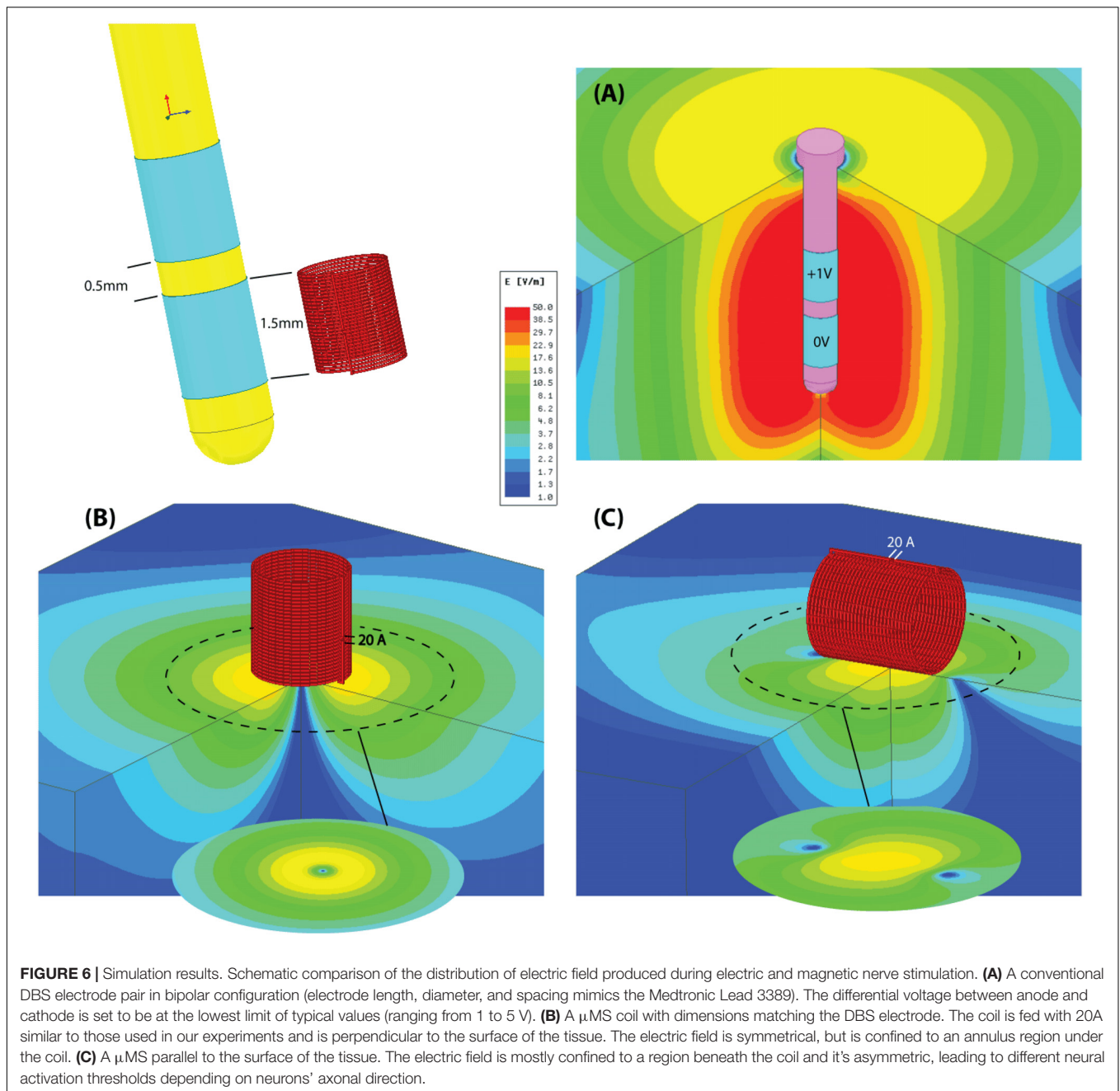
Electrophysiology

Recordings were conducted at multiple sites along the tonotopic axis of the central nucleus of the contralateral IC. This region was recognized by its sharp tuning properties and by the progression from high to low-frequency selectivities as the electrode was moved along the dorsoventral axis. Methods for recording and analyzing multiunit signals were similar to those described in

previous studies (Manzoor et al., 2012, 2013). Signals were filtered and amplified using an Alpha Omega (SNR, Alpha Omega, Inc., Nazareth, Israel) preamplifier. Neural signals were digitized and read off the electrode channels using a National Instruments data acquisition board and customized software written in MATLAB Software was used to synchronize data collection with acoustic stimulus delivery for tuning curve and rate vs. tone level testing and with magnetic stimulus delivery. The software also allowed selection of stimulus parameters to test stimulus–response relationships.

Acoustic Stimulation

Acoustic stimuli were needed for the dual purposes of characterizing the frequency tuning properties of recorded neurons to determine tonotopic coordinates of the IC recording



electrodes, and also to examine effects of changing the acoustic stimulus conditions on IC responses. For both measures, we used 40 ms tone bursts (5 ms rise/fall times, 40 ms interstimulus intervals). For testing the tuning properties, we used a battery of 800 tone bursts varied in frequency from 3 to 32 kHz and in intensity from 6 to 96 dB SPL as previously described (Finlayson and Kaltenbach, 2009).

Data Analysis

Samples of activity recorded from IC neurons were obtained from 100 to 150 repetitive stimuli and plotted as a function of time. The resulting time sweeps were used to compare responses

during and following stimulation with the activity level recorded during the prestimulus period and to derive measures of several response characteristics, such as amplitude and magnetic coil orientation. Each of these measures was obtained for each of the parameters of stimulation that were tested and were compared with responses to baseline activities stimulation. Specifically, for each stimulation parameter (Amplitude and Orientation) baseline activities (15 ms before each stimulation pulse) were compared to stimulation response (15 ms following stimulation artifact; 17–32 ms). To facilitate comparisons, the absolute value of raw electrophysiological activities were summed for the baseline and stimulus–response periods for each stimulus

delivered. Significant differences in responses for each parameter were compared using parametric ANOVA with Bonferroni corrections. In each analysis, responses were compared to their baseline activities and then tested relative to each amplitude or orientation.

RESULTS

We have explored the effects of coil orientation on the resulting stimulation capabilities both with numerical simulations and with animal studies.

Numerical Simulations

The use of magnetic fields to induce electric fields or currents in the tissue from a distance is extremely inefficient from an energy standpoint. We hypothesize that much smaller energy than TMS may be required for neural stimulation at a microscopic level. One important difference between \vec{E} and \vec{H} is that the magnitude of the latter is well-known to fall much more rapidly in space (e.g., quadratic vs. cubic law for an electric vs. magnetic dipole in empty space). Our hypothesis is based on the prediction by various activation models (Warman et al., 1992) that the gradient of the E field, is primarily responsible for neural stimulation. The FEM simulations confirm that the electric field gradient (i.e., 10^5 V/m²) induced by a peak voltage of 35 V driven μ MS in the physiological solution at the distances of 20 μ m below the microcoil is comparable to the electric field gradient (i.e., 7.6×10^5 V/m²) generated by a stimulation peak voltage of 5 V driven DBS electrode set (Astrom et al., 2015). In contrast, the electric field gradient sensitivity threshold for peripheral nerve stimulation in MRI (Koshtoiants Kh, 1957; Schaefer et al., 2000; Bencsik et al., 2007) is much smaller (Blake et al., 2014) (i.e., 150 V/m²) and can become near zero in quasi-uniform electric field modes such as in TMS (Barker et al., 1985; Bikson et al., 2013), given distance between the coil and the stimulated target region, which is referred to as the electric “farfield.” This farfield is hypothesized to produce stimulation through bends of the axon’s trajectory (Sheikh-Zade et al., 1987). Thus, the neuronal stimulation mode based on electric field gradient or “nearfield” is dominant for μ MS, albeit farfield or combination of these two modes may also play a role for neurons further away.

The FEM simulations also predict that solenoidal μ MS coils placed parallel to the surface of the tissue are capable of differentially activating neurons based on their axonal direction. It is established that neural activation function is proportional to the spatial derivative of the electric field along the axon’s axis (Roth and Basser, 1990). Our electromagnetic simulations predicted that the spatial derivative of electric field reached values up to three times higher for axons orientated in parallel-orthogonal orientation than for those oriented in parallel-parallel position (Figure 5, top). Similarly, NEURON simulations predicted that the axons whose direction is perpendicular to the long axis of the coil have a lower threshold compared to the axons parallel to the coil (Figure 5, bottom). The reason for lower threshold underneath the microcoil is that when the axons are parallel to the induced electric field the axonal activation

is maximized since the activating function of an axon is the spatial derivative of the induced electric field along the axon. On the contrary, when the axonal direction is perpendicular to the induced electric field, the gradient of the electric field along the axonal direction becomes very small. Therefore, perpendicular coil orientation requires a much higher current threshold for the axonal activation underneath the coil. However, on the edges of the microcoil, there is a sudden change in the induced electric field due to its small size resulting in the increased activating function.

Importantly, and as demonstrated here, μ MS provides a unique opportunity over electrical stimulation techniques in that neural interfaces can be constructed that take advantage of the orientation properties provided by magnetic stimulation. Namely, the construction of brain stimulation leads that maximally activate the target tissue while mitigating the activation of fibers in the passage would have a significant advantage in DBS therapies, as the activation of fibers of passage represents the greatest side-effects for patients. Likewise, μ MS coils could be used to provide more spatial resolution over existing electrical stimulation strategies, by designing interfaces that account for the orientation of the coils relative to the target tissue to be activated. This can be better appreciated from Figure 6, illustrating the schematic of the electric field distribution produced by (A) a conventional DBS electrode pair in bipolar configuration and (B,C) same-sized μ MS coils in perpendicular and parallel positions. It can be observed from the figure that even for a DBS voltage as low as 1 V (typical values range from 1 to 5 V) the electric field produced by the electrode pair covers a large symmetric area containing both electrode contacts. The electric field of the μ MS coil on the other hand, is more confined to the edges at the periphery of the coil when the coil is perpendicular to the tissue, and to the center of the solenoid when the coil is parallel to the tissue. Specifically, when the coil is in parallel position the induced electric field is asymmetric, indicating different sensitivity for neuron activation depending on their axonal direction. Moreover, we speculate that our modeling also brings up the notion that the mechanisms of action of magnetic stimulation may be fundamentally different from that of electrical stimulation. Specifically, the ionic movement of charge that ultimately results in neuronal activation operates differently between magnetic and electrical stimulation. In electrical stimulation, the current flow from pole to pole of the electrical stimulator while in magnetic stimulation the induced current flows as eddy currents relative to the magnetic fields. Electrical stimulation activates neural elements by operating on the electric potential of the extracellular matrix and manipulating the transmembrane potentials. In contrast, eddy currents act not only upon the extracellular matrix but also on the intracellular matrix as the magnetic stimulation fields penetrate the cellular compartments.

In general, μ MS operates similarly to TMS generating time-varying magnetic fields and inducing electric fields in the brain, which can stimulate surrounding cortical or subcortical neurons (Walsh and Cowey, 2000), albeit at a microscopic scale. As TMS, which is presently the method of choice to investigate causal functional interactions across macroscopic brain regions, μ MS

can be used to investigate microscopic neuronal interactions at a cell level and as such can further the aim of developing innovative technologies to understand the human brain and treat its disorders.

Animal Experiments

Recently it has been demonstrated that μ MS is capable of eliciting neuronal activation in both retinal ganglion cells *in vitro* (Bonmassar et al., 2012) and IC neurons *in vivo* (Park et al., 2013). In the *in vitro* experiments, performed in a retinal cell preparation, it was demonstrated that neuron action potentials could be elicited by μ MS. It was also demonstrated that neuronal activation was amplitude dependent, where higher amplitudes of stimulation resulted in greater activation. Also, the orientation of the coils relative to the neural substrate resulted in a different activation pattern, where perpendicular orientations of the coil resulted in minimal activation and parallel orientations resulted in maximal activation. In the *in vivo* experiments, it was demonstrated that μ MS of the DCN resulted in the generation of neuronal activities in the IC and in the cochlea. The *in vivo* experiments have recently been extended to the feline cochlea (Lee and Fried, 2017). Hence, μ MS can elicit neuronal activation within an interconnected neural circuit and is not restricted to modulation of only local circuitry. Despite these results, some key issues need to be addressed before μ MS can be further translated to chronic neuromodulation therapies, including the effect of coil orientation *in vivo* experiments.

The microcoil prototypes we tested in this study reproducibly activated the brain, *in vivo*, in a tissue-appropriate manner consistent with the known microcircuitry of the DCN and projection patterns that link the DCN to the IC. Two adult male Syrian golden hamsters were studied, and all surgical procedures used to expose the DCN and IC were the same as previously described (Manzoor et al., 2012, 2013). The microcoils produced responses that were typically manifested in the contralateral IC as bursts or barrages of spike-like waveforms in the first 15–20 ms of the post-stimulus period (Figure 7). The responses to the microcoils placed just above but not in contact with the DCN surface produced well-defined activity that resembled the spike-like multiunit responses observed during sound stimulation (Kaltenbach and McCaslin, 1996; Kaltenbach and Afman, 2000).

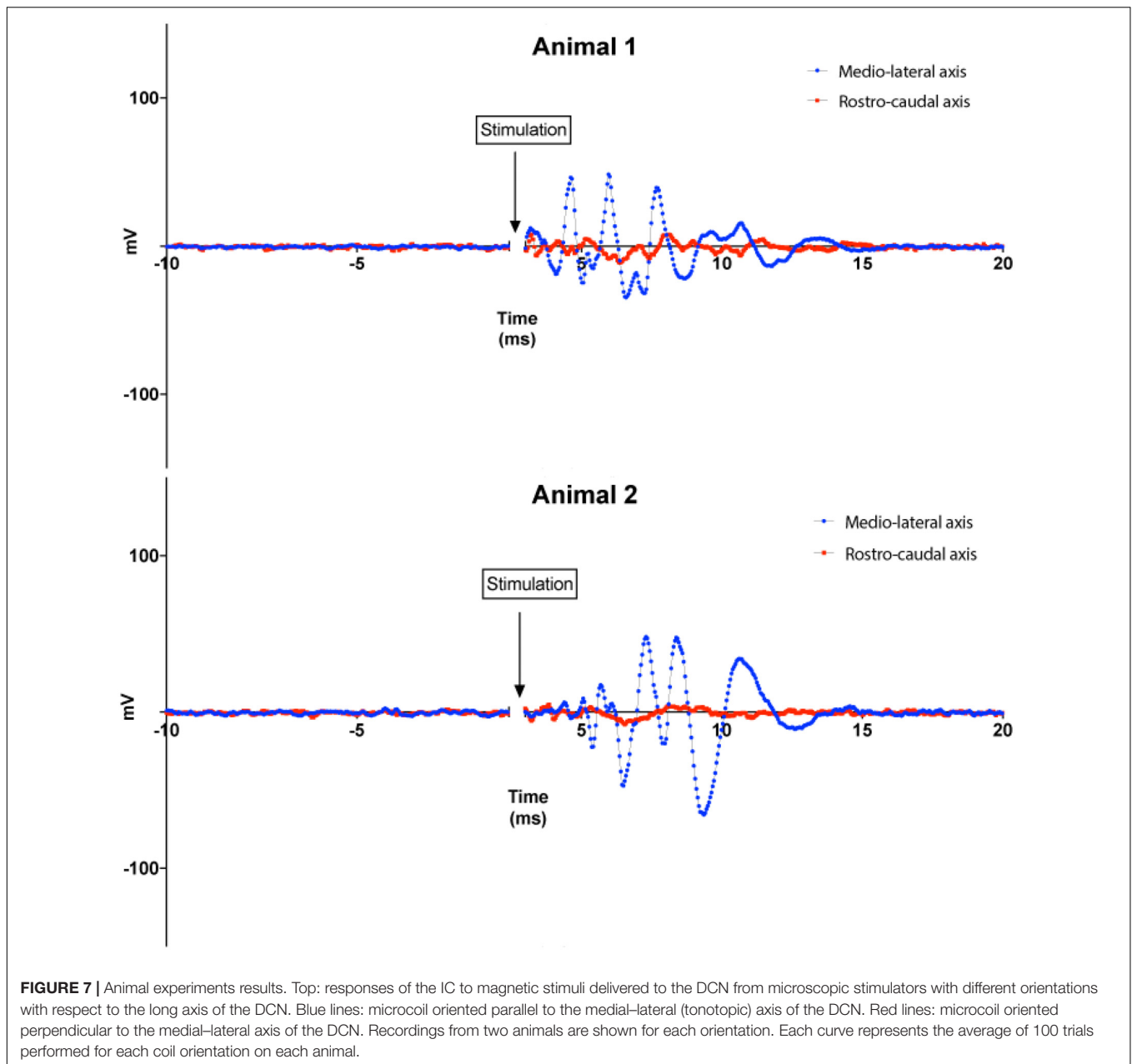
In a set of experiments, we examined the effect of coil orientation on neuronal activation properties. Two different orientations of the microcoils were studied, one with the long axis of the μ MS parallel to the long (medial–lateral or tonotopic) axis of the DCN (Figure 3, bottom), and the other with the long axis of the μ MS coil parallel to the rostrocaudal axis of the DCN (i.e., parallel to the isofrequency bands) (Figure 3, bottom). Strong IC responses were observed for microcoil orientations parallel to the medial–lateral axis of the DCN, while weaker or absent responses for the orthogonal orientations (Figure 7, top). In animal 2 (Figure 7, bottom), both the medial–lateral orientations were different from the rostral–caudal orientation but were not different from animal 1.

An important aspect of our results that was unexpected was the dependence of the strength of the IC response on the rotational angle of the microcoil above the DCN. IC responses

were vigorous when the long axis of the microcoil was parallel to the medial–lateral axis of the DCN but weak for micro-stimulator orientations parallel to the rostrocaudal axis. This difference implies contrasting levels of efficacy in stimulus–response coupling between the different micro-stimulator orientations. The simplest mechanism to explain this results is that micro-stimulator orientations parallel to the medial–lateral axis of the DCN more effectively excite the main output neurons of the DCN, the fusiform cells, which project to the contralateral IC (Beyerl, 1978; Ryugo and Willard, 1985; Cant and Benson, 2003). This greater effectiveness of activation may occur because any stimulation that fusiform cells receive may receive input directly from the fibers running along the tonotopic columns of the DCN that are activated by the microcoil in the medial–lateral axis orientation (Mugnaini et al., 1980; Blackstad et al., 1984; Manis, 1989; Kanold and Young, 2001) and potentiate the responses of fusiform cells to other inputs (Fujino and Oertel, 2003; Tzounopoulos et al., 2007). Activation of fibers running along the tonotopic column would be expected to be greater when the axis of the micro-stimulator is perpendicular to the axes of the tonotopic column, thus parallel to the medial–lateral axis, as shown by our numerical simulations results. At the present juncture, we have not yet elucidated precise targets of the stimulation of the DCN circuitry. Multiple neural populations in the ventral cochlear nucleus (VCN) also project to the IC and interact with the DCN circuitry as well. These polysynaptic pathways are potential targets and possibly underlie the generation of late-onset responses in the IC.

DISCUSSION

There are some limitations that currently limit the efficacy and safety of electrical stimulation. First, electric currents delivered by microelectrodes can spread to undesired areas adjacent to the targeted structures, leading to unintended side effects (Histed et al., 2009; Behrend et al., 2011; Licari et al., 2011; Weitz et al., 2015). For example, imprecise targeting of the subthalamic nucleus (STN) due to current spread to neighboring white matter tracts during DBS in Parkinson's patients can lead to undesirable motor and sensory responses (Li et al., 2016). In this work, we show that unlike electrical stimulation μ MS has the potential of being able to stimulate target nuclei in the brain without affecting the surrounding white matter tracts. Neuronal processes such as axons parallel to the direction of the electric current density \vec{j} are depolarized or hyperpolarized depending on the direction and strength of \vec{j} , but the processes transverse to the \vec{j} are not affected (Beurrier et al., 2001). Thus, the magnetic stimulation via μ MS is capable of synaptically activating or inhibiting neurons in a spatially oriented manner. One aspect of the directionality of μ MS was shown *in vitro* (Serano et al., 2015), where depending on the direction of the magnetic field flux the axon of the ganglion cell beneath the coil showed the generation of action potentials recorded by the patch clamping technique. In this work, we also expand this finding to our *in vivo* rodent model, showing for the first time, our ability to stimulate the brain stem of a rodent with a net sensitivity



to the directionality of the magnetic flux. A similar μ MS-orientation sensitivity was shown (Lee and Fried, 2017) in layer V pyramidal neurons (PNs) and the asymmetric fields arising from such microcoils did not simultaneously activate horizontally oriented axon. Furthermore, μ MS was shown to stimulate in confined narrow regions ($<60 \mu\text{m}$) cortical pyramidal neurons in brain slices *in vitro*, which helped to avoid the simultaneous activation of passing axons (Mehta and Oxenham, 2017). μ MS coils were also surgically introduced 8–10 mm into the cochlea of anesthetized deafened felines (Lee and Fried, 2017), thus unresponsive to acoustic stimuli, and auditory responses were then recorded during magnetic stimulation. These experiments were aimed at showing that magnetic field steerability of μ MS

may solve the low-resolution stimulation shortcomings of the state-of-the-art cochlear implants that are limited by their ability to reproduce accurately pitch in music and speech in the presence of background noise, which instead may require as much as four times the number of channels currently available (Mehta and Oxenham, 2017). In the cochlea (Macherey and Carlyon, 2014) as well as in cortex (Matteucci et al., 2016) stimulation resolution is limited by the channel to channel cross-talk rather than electrode sub-millimeter size and spacing. μ MS has shown the ability to selectively activate neurons by different orientations, thus a μ MS coil in a single position can activate different neurons by rotation, thus increasing the spatial resolution.

Second, unlike electrical stimulation, μ MS does not require direct galvanic contact with the tissue. For an electrode pair (Figure 1A) to generate current, it needs to be placed in direct contact with a conductive media (e.g., excitable tissue). In a bipolar electrode pair, the ‘anode’ or source (Figure 1A, plus sign) injects a current and hyperpolarizes the neuronal membrane toward more negative potential which can arrest the neural action, whereas the ‘cathode’ acts as a sink and depolarizes the axon membrane which could trigger an action potential (Figure 1A, minus sign). However, the metal electrode implanted in the tissue may lead to oxidation–reduction reaction at the electrode-tissue interface changing the pH of surrounding tissue which may provoke an immune response. Histopathology analysis has shown gliosis and spongiosis around the stimulation electrode track (Caparros-Lefebvre et al., 1994), which formed an encapsulation layer referred to as the “glial scar.” With μ MS however, the solenoidal coil (Figures 1B–D) can induce a current from a distance, without placing a metal in direct contact with the tissue and new materials may allow for soft coils development (Wang et al., 2000). The pulsed current passing through the coil generates a time-varying magnetic field B inside and in the space surrounding the coil. In the conductive tissue, this time-varying magnetic field \vec{B} , in turn, generates an orthogonal current density \vec{J} capable of evoking neuronal action potentials (Figures 1B–D), according to Faraday’s Law [i.e., $\frac{1}{\sigma} \nabla \times \vec{J} = -\frac{\partial \vec{B}}{\partial t}$ in homogeneous isotropic medium where $\nabla \times$ is the curl operator and σ is, the tissue conductivity, albeit the brain has tissues with anisotropic conductivities (Tuch et al., 1999)]. A number of studies have shown that the magnetically induced currents can directly excite axons as long as the spatial gradient of the induced electric field is strong enough to generate a transmembrane potential above the threshold (Roth and Basser, 1990; Basser and Roth, 1991; Pashut et al., 2011). The exact threshold depends on the axon’s geometry such as the diameter and its geometrical shape (Pashut et al., 2011), the pulse width (Basser and Roth, 1991), size and shape of the electrodes, etc. Furthermore, even though electric stimulation affects the myelinated neurons in the nodes of Ranvier, μ MS can theoretically stimulate a myelinated axon anywhere within its length. Modulation of neuronal activation or inhibition can also be potentially achieved in μ MS by driving specific waveforms (e.g., sharp rising edges followed by slowly falling dips, and vice versa), producing asymmetric induced current pulses in the tissue.

Finally, unlike electrical stimulation μ MS does not require a charge-balanced stimulation waveform. In electrical stimulation, charge balancing is necessary to avoid excessive charge accumulation at the neural interface, and thus undesired stimulation and electroporation (Nduka et al., 2017). Electroporation occurs when the external electric field of the membrane potential of the cell exceeds a 0.2–1 V threshold, which leads to a change in the molecular structure of the membrane, and a subsequent membrane perforation with pore formation increasing the membrane permeability to ions, and molecules (Chen et al., 2006). Electroporation with a transmembrane potential of approximately 1 V could cause necrosis, due to membrane rupture and the subsequent

cytoplasmic contents leakage (Sale and Hamilton, 1968; Neumann and Rosenheck, 1972; Crowley, 1973). In μ MS, no net charge is transferred from the electrode into tissue since neither sinks nor sources are present when a current density \vec{J} is induced by the time-varying magnetic field. The current density in the tissue \vec{J} is a rotating field that mirrors the current direction in the coil (Figure 1B). Because the induced electric field is a solenoidal or incompressible vector field in three dimensions, μ MS does not suffer from charge buildup (Bonmassar et al., 2012).

Despite these specific limitations, electrically based DBS has been tremendously successful. However, the application of μ MS could mitigate some of the challenges of these limitations. Theoretically, and supported by limited data (Bonmassar et al., 2012), it is possible that specific orientations of magnetic fields relative to different neural substrates may result in differential neuronal response patterns. If demonstrated to be a valid property of magnetic stimulation, this would open the possibility of custom designing μ MS coils in a way to maximize the stimulation of the intended target and minimizing the activation of unintended targets. In the case of DBS for movement disorders, the primary cause of side-effects is the unintended activation of fibers of passage. Namely, with STN stimulation the activation of the internal capsule, adjacent and lateral to the STN, or activation of the medial lemniscus fibers, medial to the STN, can cause muscle contracts or paresthesia respectively. Even if therapeutic efficacy is seen in a patient, it is possible that activation of these fibers of passage can limit the ultimate therapeutic effect, as the threshold of the side-effect may be less than the threshold for therapeutic benefit. The unintended activation of fibers of the passage is not unique to STN stimulation, as the unintended activation of the internal capsule is also seen with DBS of the ventral intermediate nucleus of the thalamus and globus pallidus internus, which are the other primary targets for DBS therapy for Parkinson’s disease. Hence, if it is demonstrated that orientation of magnetic fields has differential effects on the activation of axonal fibers, one can propose to custom design μ MS coils to take advantage of this unique property. As this property is not directly achievable with electrical stimulation based technologies, it would provide a new avenue to improve outcomes and mitigate side-effects beyond the other limitation previously discussed between electrical and magnetic stimulation based approaches.

CONCLUSION

Microscopic magnetic stimulation (μ MS) could potentially become the pacemaker and brain stimulator of the future with their contactless ability to deliver the neuronal stimulation needed for therapeutic efficacy in patients with Parkinson’s disease, epilepsy, in need of implantable cardioverter-defibrillators or pacemakers, and so forth. Due to recent advancements in micro-machining technologies, we can now utilize manufactured inductors (or coils) constructed on the sub-millimeter scale to produce magnetic fields. Such coils would offer several advantages over classical electrical and TMS

techniques. Unlike TMS coils, the coils are sub-millimeter in size and can be placed within or near a neuronal substrate, increasing spatial resolution and reducing the power needed to evoke neuronal activity. Moreover, because the coils are not in direct contact with the tissue and no current is directly injected into the tissue, they may overcome the inflammatory tissue encapsulation and mitigate charge buildup issues inherent in traditional electrical stimulation technologies. Our data indicate that these microcoils can activate neuronal activity with high degrees of spatial and temporal resolution and that the orientation of the coils relative to the tissue activated can be used to activate specific elements optimally and to avoid the activation of others. Future work will concentrate on developing specific neural models of the target structures to quantify the parameters of μ MS for directional stimulation, and include more animal models to establish the statistical features of the neural response.

ETHICS STATEMENT

This study was carried out in accordance with the recommendations of Public Health Service (PHS) Policy on

Humane Care and Use of Laboratory Animals and the Animal Welfare Act. The protocol was approved by the institutional animal care and use committee (IACUC) Committee of the Cleveland Clinic.

AUTHOR CONTRIBUTIONS

LaG, JG, JK, and GB conceptualized the study; provided support and guidance with data interpretation. H-JP designed and performed the NEURON analyses with support from LaG and JK. NM and LyG designed and performed the animal experiments with support from JK and H-JP. LaG and GB contributed electromagnetics data analysis and visualization software. FH built the μ MS coils. LaG wrote the manuscript, with contributions from GB and comments from all other authors.

FUNDING

This work was supported by the US National Institutes of Health (NIH) grants R43MH107037 (FH, JG, GB, and JK), R01MH111875 (GB), and K99EB021320 (LaG).

REFERENCES

- Astrom, M., Diczfalusy, E., Martens, H., and Wardell, K. (2015). Relationship between neural activation and electric field distribution during deep brain stimulation. *IEEE Trans. Biomed. Eng.* 62, 664–672. doi: 10.1109/TBME.2014.2363494
- Ayton, L. N., Blamey, P. J., Guymer, R. H., Luu, C. D., Nayagam, D. A., Sinclair, N. C., et al. (2014). First-in-human trial of a novel suprachoroidal retinal prosthesis. *PLoS One* 9:e115239. doi: 10.1371/journal.pone.0115239
- Barker, A. T., Jalinous, R., and Freeston, I. L. (1985). Non-invasive magnetic stimulation of human motor cortex. *Lancet* 1, 1106–1107. doi: 10.1016/S0140-6736(85)92413-4
- Basser, P. J., and Roth, B. J. (1991). Stimulation of a myelinated nerve axon by electromagnetic induction. *Med. Biol. Eng. Comput.* 29, 261–268. doi: 10.1007/BF02446708
- Behrend, M. R., Ahuja, A. K., Humayun, M. S., Chow, R. H., and Weiland, J. D. (2011). Resolution of the epiretinal prosthesis is not limited by electrode size. *IEEE Trans. Neural Syst. Rehabil. Eng.* 19, 436–442. doi: 10.1109/TNSRE.2011.2140132
- Benabid, A. L. (2003). Deep brain stimulation for Parkinson's disease. *Curr. Opin. Neurobiol.* 13, 696–706. doi: 10.1016/j.conb.2003.11.001
- Bencsik, M., Bowtell, R., and Bowley, R. (2007). Electric fields induced in the human body by time-varying magnetic field gradients in MRI: numerical calculations and correlation analysis. *Phys. Med. Biol.* 52, 2337–2353. doi: 10.1088/0031-9155/52/9/001
- Beurrier, C., Bioulac, B., Audin, J., and Hammond, C. (2001). High-frequency stimulation produces a transient blockade of voltage-gated currents in subthalamic neurons. *J. Neurophysiol.* 85, 1351–1356. doi: 10.1152/jn.2001.85.4.1351
- Beyerl, B. D. (1978). Afferent projections to the central nucleus of the inferior colliculus in the rat. *Brain Res.* 145, 209–223. doi: 10.1016/0006-8993(78)90858-2
- Bikson, M., Dmochowski, J., and Rahman, A. (2013). The “quasi-uniform” assumption in animal and computational models of non-invasive electrical stimulation. *Brain Stimul.* 6, 704–705. doi: 10.1016/j.brs.2012.11.005
- Blackstad, T. W., Osen, K. K., and Mugnaini, E. (1984). Pyramidal neurones of the dorsal cochlear nucleus: a Golgi and computer reconstruction study in cat. *Neuroscience* 13, 827–854. doi: 10.1016/0306-4522(84)90099-X
- Blake, D. T., Bhatti, P. T., Beek-King, J. V., Crawford, J., and McKinnon, B. (2014). “Micro magnetic stimulation of the feline cochlea,” in *Proceedings of the 13th International Conference on Cochlear Implants and Other Implantable Auditory Technologies*, Munich, S4–S8.
- Bonmassar, G., Lee, S. W., Freeman, D. K., Polasek, M., Fried, S. I., and Gale, J. T. (2012). Microscopic magnetic stimulation of neural tissue. *Nat. Commun.* 3:921. doi: 10.1038/ncomms1914
- Butson, C. R., and McIntyre, C. C. (2006). Role of electrode design on the volume of tissue activated during deep brain stimulation. *J. Neural Eng.* 3, 1–8. doi: 10.1088/1741-2560/3/1/001
- Cant, N. B., and Benson, C. G. (2003). Parallel auditory pathways: projection patterns of the different neuronal populations in the dorsal and ventral cochlear nuclei. *Brain Res. Bull.* 60, 457–474. doi: 10.1016/S0304-9230(03)00050-9
- Caparros-Lefebvre, D., Ruchoux, M. M., Blond, S., Petit, H., and Percheron, G. (1994). Long-term thalamic stimulation in Parkinson's disease: postmortem anatomoclinical study. *Neurology* 44, 1856–1860. doi: 10.1212/WNL.44.10.1856
- Carnevale, N. T., and Hines, M. L. (2006). *The Neuron Book*. Cambridge: Cambridge University Press. doi: 10.1017/CBO9780511541612
- Chen, C., Smye, S. W., Robinson, M. P., and Evans, J. A. (2006). Membrane electroporation theories: a review. *Med. Biol. Eng. Comput.* 44, 5–14. doi: 10.1007/s11517-005-0020-2
- Clare McElcheran, L. G., and Graham, S. (2014). “Reduced heating of implanted electrical conductors using parallel radiofrequency transmission,” in *Proceedings of the Joint Annual Meeting of the International Society of Magnetic Resonance in Medicine (ISMRM)*, Milan.
- Condon, B., and Hadley, D. M. (2000). Potential MR hazard to patients with metallic heart valves: the Lenz effect. *J. Magn. Reson. Imaging* 12, 171–176. doi: 10.1002/1522-2586(200007)12:1<171::AID-JMRI19>3.0.CO;2-W
- Crowley, J. M. (1973). Electrical breakdown of bimolecular lipid membranes as an electromechanical instability. *Biophys. J.* 13, 711–724. doi: 10.1016/S0006-3495(73)86017-5
- Deng, Z.-D., Lisanby, S. H., and Peterchev, A. V. (2013). Electric field depth-focality tradeoff in transcranial magnetic stimulation: simulation comparison of 50 coil designs. *Brain Stimul.* 6, 1–13. doi: 10.1016/j.brs.2012.02.005
- Deuschl, G., Schade-Brittinger, C., Krack, P., Volkmann, J., Schäfer, H., Bötzel, K., et al. (2006). A randomized trial of deep-brain stimulation for Parkinson's disease. *N. Engl. J. Med.* 355, 896–908. doi: 10.1056/NEJMoa060281
- Ellenbogen, K. A., and Wood, M. A. (2008). *Cardiac Pacing and ICDs*, 5th Edn, Vol. IX. Hoboken, NJ: Blackwell Publishing, 558.

- Finlayson, P. G., and Kaltenbach, J. A. (2009). Alterations in the spontaneous discharge patterns of single units in the dorsal cochlear nucleus following intense sound exposure. *Hear. Res.* 256, 104–117. doi: 10.1016/j.heares.2009.07.006
- Fujino, K., and Oertel, D. (2003). Bidirectional synaptic plasticity in the cerebellum-like mammalian dorsal cochlear nucleus. *Proc. Natl. Acad. Sci. U.S.A.* 100, 265–270. doi: 10.1073/pnas.0135345100
- Gifford, R. H. (2013). *Cochlear Implant Patient Assessment: Evaluation of Candidacy, Performance, and Outcomes. Core Clinical Concepts in Audiology*. San Diego, CA: Plural Publishing, 144.
- Golestani-Rad, L., Elahi, B., and Rashed-Mohassel, J. (2007). Investigating the effects of external fields polarization on the coupling of pure magnetic waves in the human body in very low frequencies. *Biomagn. Res. Technol.* 5:3. doi: 10.1186/1477-044X-5-3
- Golestanirad, L., Dlala, E., Wright, G., Mosig, J. R., and Graham, S. J. (2012a). Comprehensive analysis of Lenz Effect on the artificial heart valves during magnetic resonance imaging. *Prog. Electromagn. Res.* 128, 1–17. doi: 10.2528/PIER12031505
- Golestanirad, L., Elahi, B., Molina, A., Mosig, J. R., Pollo, C., Chen, R., et al. (2013). Analysis of fractal electrodes for efficient neural stimulation. *Front. Neuroeng.* 6:3. doi: 10.3389/fneng.2013.00003
- Golestanirad, L., Iacono, M. I., Keil, B., Angelone, L. M., Bonmassar, G., Fox, M. D., et al. (2017a). Construction and modeling of a reconfigurable MRI coil for lowering SAR in patients with deep brain stimulation implants. *Neuroimage* 147, 577–588. doi: 10.1016/j.neuroimage.2016.12.056
- Golestanirad, L., Izquierdo, A. P., Graham, S. J., Mosig, J. R., and Pollo, C. (2012b). Effect of realistic modeling of deep brain stimulation on the prediction of volume of activated tissue. *Prog. Electromagn. Res.* 126, 1–16. doi: 10.2528/PIER12013108
- Golestanirad, L., Keil, B., Angelone, L. M., Bonmassar, G., Mareyam, A., and Wald, L. L. (2017b). Feasibility of using linearly polarized rotating birdcage transmitters and close-fitting receive arrays in MRI to reduce SAR in the vicinity of deep brain stimulation implants. *Magn. Reson. Med.* 77, 1701–1712. doi: 10.1002/mrm.26220
- Golestanirad, L., Mattes, M., Mosig, J. R., and Pollo, C. (2010). Effect of model accuracy on the result of computed current densities in the simulation of transcranial magnetic stimulation. *IEEE Trans. Magn.* 46, 4046–4051. doi: 10.1109/TMAG.2010.2082556
- Golestanirad, L., Rouhani, H., Elahi, B., Shahim, K., Chen, R., Mosig, J. R., et al. (2012c). Combined use of transcranial magnetic stimulation and metal electrode implants: a theoretical assessment of safety considerations. *Phys. Med. Biol.* 57:7813. doi: 10.1088/0031-9155/57/23/7813
- Histed, M. H., Bonin, V., and Reid, R. C. (2009). Direct activation of sparse, distributed populations of cortical neurons by electrical microstimulation. *Neuron* 63, 508–522. doi: 10.1016/j.neuron.2009.07.016
- Howland, R. H. (2008). Neurosurgical approaches to therapeutic brain stimulation for treatment-resistant depression. *J. Psychosoc. Nurs. Ment. Health Serv.* 46, 15–19.
- Humayun, M. S., Dorn, J. D., da Cruz, L., Dagnelie, G., Sahel, J. A., Stanga, P. E., et al. (2012). Interim results from the international trial of Second Sight's visual prosthesis. *Ophthalmology* 119, 779–788. doi: 10.1016/j.ophtha.2011.09.028
- Johnson, M. D., and McIntyre, C. C. (2008). Quantifying the neural elements activated and inhibited by globus pallidus deep brain stimulation. *J. Neurophysiol.* 100, 2549–2563. doi: 10.1152/jn.90372.2008
- Kaltenbach, J. A., and Afman, C. E. (2000). Hyperactivity in the dorsal cochlear nucleus after intense sound exposure and its resemblance to tone-evoked activity: a physiological model for tinnitus. *Hear. Res.* 140, 165–172. doi: 10.1016/S0378-5955(99)00197-5
- Kaltenbach, J. A., and McCaslin, D. L. (1996). Increases in spontaneous activity in the dorsal cochlear nucleus following exposure to high intensity sound: a possible neural correlate of tinnitus. *Audit. Neurosci.* 3, 57–78.
- Kanold, P. O., and Young, E. D. (2001). Proprioceptive information from the pinna provides somatosensory input to cat dorsal cochlear nucleus. *J. Neurosci.* 21, 7848–7858. doi: 10.1523/JNEUROSCI.21-19-07848.2001
- Koshtoiants Kh, S. (1957). Enzymo-chemical principles of the action of the vagus nerve on the heart (role of potassium). *Fiziol. Zh. SSSR Im. I M Sechenova* 43, 681–684.
- Kreis, P., and Fishman, S. (2009). *Spinal Cord Stimulation Implantation Percutaneous Implantation Techniques*. Oxford: Oxford Press.
- Lee, S. W., and Fried, S. I. (2017). Enhanced control of cortical pyramidal neurons with micromagnetic stimulation. *IEEE Trans. Neural Syst. Rehabil. Eng.* 25, 1375–1386. doi: 10.1109/TNSRE.2016.2631446
- Li, Z., Zhang, J. G., Ye, Y., and Li, X. (2016). Review on factors affecting targeting accuracy of deep brain stimulation electrode implantation between 2001 and 2015. *Stereotact. Funct. Neurosurg.* 94, 351–362. doi: 10.1159/000449206
- Licari, F. G., Shkoukani, M., and Kaltenbach, J. A. (2011). Stimulus-dependent changes in optical responses of the dorsal cochlear nucleus using voltage-sensitive dye. *J. Neurophysiol.* 106, 421–436. doi: 10.1152/jn.00982.2010
- Lopez, W. O., Barbosa, D. C., Teixeira, M. J., Paiz, M., Moura, L., Monaco, B. A., et al. (2016). Pain relief in CRPS-II after spinal cord and motor cortex simultaneous dual stimulation. *Pain Phys.* 19, E631–E635.
- Macherey, O., and Carlyon, R. P. (2014). Cochlear implants. *Curr. Biol.* 24, R878–R884. doi: 10.1016/j.cub.2014.06.053
- Manis, P. B. (1989). Responses to parallel fiber stimulation in the guinea pig dorsal cochlear nucleus in vitro. *J. Neurophysiol.* 61, 149–161. doi: 10.1152/jn.1989.61.1.149
- Manzoor, N. F., Gao, Y., Licari, F., and Kaltenbach, J. A. (2013). Comparison and contrast of noise-induced hyperactivity in the dorsal cochlear nucleus and inferior colliculus. *Hear. Res.* 295, 114–123. doi: 10.1016/j.heares.2012.04.003
- Manzoor, N. F., Licari, F. G., Klapchar, M., Elkin, R. L., Gao, Y., Chen, G., et al. (2012). Noise-induced hyperactivity in the inferior colliculus: its relationship with hyperactivity in the dorsal cochlear nucleus. *J. Neurophysiol.* 108, 976–988. doi: 10.1152/jn.00833.2011
- Matteucci, P. B., Barriga-Rivera, A., Eiber, C. D., Lovell, N. H., Morley, J. W., and Suaning, G. J. (2016). The effect of electric cross-talk in retinal neurostimulation. *Invest. Ophthalmol. Vis. Sci.* 57, 1031–1037. doi: 10.1167/iov.15-18400
- McElcheran, C. E., Yang, B., Anderson, K. J. T., Golestanirad, L., and Graham, S. J. (2017). Parallel radiofrequency transmission at 3 tesla to improve safety in bilateral implanted wires in a heterogeneous model. *Magn. Reson. Med.* 78, 2406–2415. doi: 10.1002/mrm.26622
- McIntyre, C. C., and Grill, W. M. (2001). Finite element analysis of the current-density and electric field generated by metal microelectrodes. *Ann. Biomed. Eng.* 29, 227–235. doi: 10.1114/1.1352640
- McIntyre, C. C., Mori, S., Sherman, D. L., Thakor, N. V., and Vitek, J. L. (2004). Electric field and stimulating influence generated by deep brain stimulation of the subthalamic nucleus. *Clin. Neurophysiol.* 115, 589–595. doi: 10.1016/j.clinph.2003.10.033
- McIntyre, C. C., Richardson, A. G., and Grill, W. M. (2002). Modeling the excitability of mammalian nerve fibers: influence of afterpotentials on the recovery cycle. *J. Neurophysiol.* 87, 995–1006. doi: 10.1152/jn.00353.2001
- Mehta, A. H., and Oxenham, A. J. (2017). Vocoder simulations explain complex pitch perception limitations experienced by cochlear implant users. *J. Assoc. Res. Otolaryngol.* 18, 789–802. doi: 10.1007/s10162-017-0632-x
- Møller, A. R. (2006). *Cochlear and Brainstem Implants. Advances in Oto-Rhino-Laryngology*, Vol. VIII. New York, NY: Karger, 228. doi: 10.1159/isbn.978-3-318-01380-1
- Montgomery, E. B. (2010). *Deep Brain Stimulation Programming: Principles and Practice*, Vol. XVII. Oxford: Oxford University Press, 179.
- Morace, R., Di Gennaro, G., Quarato, P., D'Aniello, A., Amascia, A., Grammaldo, L., et al. (2016). Deep brain stimulation for intractable epilepsy. *J. Neurosurg.* 124, 189–198.
- Mugnaini, E., Warr, W. B., and Osen, K. K. (1980). Distribution and light microscopic features of granule cells in the cochlear nuclei of cat, rat, and mouse. *J. Comp. Neurol.* 191, 581–606. doi: 10.1002/cne.901910406
- Nagarajan, S. S., Durand, D. M., and Warman, E. N. (1993). Effects of induced electric fields on finite neuronal structures: a simulation study. *IEEE Trans. Biomed. Eng.* 40, 1175–1188. doi: 10.1109/10.245636
- Nduka, C. C., Poland, N., Kennedy, M., Dye, J., and Darzi, A. (2017). The cutting mechanism of the electrosurgical scalpel. *J. Phys. D Appl. Phys.* 50:025401.
- Neumann, E., and Rosenheck, K. (1972). Permeability changes induced by electric impulses in vesicular membranes. *J. Membr. Biol.* 10, 279–290. doi: 10.1007/BF01867861

- O'Reardon, J. P., Cristancho, P., and Peshek, A. D. (2006). Vagus nerve stimulation (VNS) and treatment of depression: to the brainstem and beyond. *Psychiatry* 3, 54–63.
- Panayiotopoulos, C. P. (2011). *Principles of Therapy in the Epilepsies*, Vol. VIII. New York, NY: Springer, 99. doi: 10.1007/978-0-85729-009-0
- Park, H. J., Bonmassar, G., Kaltenbach, J. A., Machado, A. G., Manzoor, N. F., and Gale, J. T. (2013). Activation of the central nervous system induced by micro-magnetic stimulation. *Nat. Commun.* 4:2463. doi: 10.1038/ncomms3463
- Pashut, T., Wolfus, S., Friedman, A., Lavidor, M., Bar-Gad, I., Yeshurun, Y., et al. (2011). Mechanisms of magnetic stimulation of central nervous system neurons. *PLoS Comput. Biol.* 7:e1002022. doi: 10.1371/journal.pcbi.1002022
- Ren, Z. (2002). T-Omega formulation for eddy-current problems in multiply connected regions. *IEEE Trans. Magn.* 38, 557–560. doi: 10.1109/20.996146
- Roth, B. J., and Basser, P. J. (1990). A model of the stimulation of a nerve fiber by electromagnetic induction. *IEEE Trans. Biomed. Eng.* 37, 588–597. doi: 10.1109/10.55662
- Ryugo, D. K., and Willard, F. H. (1985). The dorsal cochlear nucleus of the mouse: a light microscopic analysis of neurons that project to the inferior colliculus. *J. Comp. Neurol.* 242, 381–396. doi: 10.1002/cne.902420307
- Sale, A. J., and Hamilton, W. A. (1968). Effects of high electric fields on micro-organisms. 3. Lysis of erythrocytes and protoplasts. *Biochim. Biophys. Acta* 163, 37–43. doi: 10.1016/0005-2736(68)90030-8
- Schaefer, D., Bourland, J., and Nyenhuis, J. (2000). Review of patient safety in time-varying gradient fields. *J. Magn. Reson. Imaging* 12, 20–29. doi: 10.1002/1522-2586(200007)12:1<20::AID-JMRI3>3.0.CO;2-Y
- Serano, P., Angelone, L. M., Katmani, H., Eskandar, E., and Bonmassar, G. (2015). A novel brain stimulation technology provides compatibility with MRI. *Sci. Rep.* 5:9805. doi: 10.1038/srep09805
- Sheikh-Zade, I. R., Kruchinin, V. M., Sukach, L. I., Pokrovskii, M. V., and Urmancheva, T. G. (1987). General principles of heart rate control during burst stimulation of the vagus nerve in various animals. *Fiziol. Zh. SSSR Im. I M Sechenova* 73, 1325–1330.
- Shepherd, R. K., Shivdasani, M. N., Nayagam, D. A., Williams, C. E., and Blamey, P. J. (2013). Visual prostheses for the blind. *Trends Biotechnol.* 31, 562–571. doi: 10.1016/j.tibtech.2013.07.001
- Stingl, K., Bartz-Schmidt, K. U., Besch, D., Chee, C. K., Cottrill, C. L., Gekeler, F., et al. (2015). Subretinal visual implant alpha IMS—clinical trial interim report. *Vision Res.* 111(Pt B), 149–160. doi: 10.1016/j.visres.2015.03.001
- Tolbert, D. L., Conoyer, B., and Ariel, M. (2004). Quantitative analysis of granule cell axons and climbing fiber afferents in the turtle cerebellar cortex. *Anat. Embryol.* 209, 49–58. doi: 10.1007/s00429-004-0423-0
- Tuch, D. S., Wedeen, V. J., Dale, A. M., George, J. S., and Belliveau, J. W. (1999). Conductivity mapping of biological tissue using diffusion MRI. *Ann. N. Y. Acad. Sci.* 888, 314–316. doi: 10.1111/j.1749-6632.1999.tb07965.x
- Tzounopoulos, T., Rubio, M. E., Keen, J. E., and Trussell, L. O. (2007). Coactivation of pre- and postsynaptic signaling mechanisms determines cell-specific spike-timing-dependent plasticity. *Neuron* 54, 291–301. doi: 10.1016/j.neuron.2007.03.026
- United States Congress Senate Committee on Finance (2006). *Committee Staff Report to the Chairman and Ranking Member: Review of the FDA's Approval Process for the Vagus Nerve Stimulation Therapy System for Treatment-Resistant Depression*. S. Prt, Vol. IV. Washington, DC: U.S. Government Printing Office, 386.
- Wagner, T., Gangitano, M., Romero, R., Théoret, H., Kobayashi, M., Ansel, D., et al. (2004). Intracranial measurement of current densities induced by transcranial magnetic stimulation in the human brain. *Neurosci. Lett.* 354, 91–94. doi: 10.1016/S0304-3940(03)00861-9
- Wagner, T. A., Zahn, M., Grodzinsky, A. J., and Pascual-Leone, A. (2004). Three-dimensional head model simulation of transcranial magnetic stimulation. *IEEE Trans. Biomed. Eng.* 51, 1586–1598. doi: 10.1109/TBME.2004.827925
- Walsh, V., and Cowey, A. (2000). Transcranial magnetic stimulation and cognitive neuroscience. *Nat. Rev. Neurosci.* 1, 73–79. doi: 10.1038/35036239
- Wang, S. X., Sun, N. X., Yamaguchi, M., and Yabukami, S. (2000). Properties of a new soft magnetic material. *Nature* 407, 150–151. doi: 10.1038/35025142
- Warman, E. N., Grill, W. M., and Durand, D. (1992). Modeling the effects of electric fields on nerve fibers: determination of excitation thresholds. *IEEE Trans. Biomed. Eng.* 39, 1244–1254. doi: 10.1109/10.184700
- Wei, X. F., and Grill, W. M. (2005). Current density distributions, field distributions and impedance analysis of segmented deep brain stimulation electrodes. *J. Neural Eng.* 2, 139–147. doi: 10.1088/1741-2560/2/4/010
- Weitz, A. C., Nanduri, D., Behrend, M. R., Gonzalez-Calle, A., Greenberg, R. J., Humayun, M. S., et al. (2015). Improving the spatial resolution of epiretinal implants by increasing stimulus pulse duration. *Sci. Transl. Med.* 7:318ra203. doi: 10.1126/scitranslmed.aac4877
- Williams, N. R., Short, E. B., Hopkins, T., Bentzley, B. S., Sahlem, G. L., Pannu, J., et al. (2016). Five-year follow-up of bilateral epidural prefrontal cortical stimulation for treatment-resistant depression. *Brain Stimul.* 9, 897–904. doi: 10.1016/j.brs.2016.06.054
- Woo, J. P., Yoo, P. B., and Grill, W. M. (2010). Finite element modeling and in vivo analysis of electrode configurations for selective stimulation of pudendal afferent fibers. *BMC Urol.* 10:11. doi: 10.1186/1471-2490-10-11
- Zrenner, E. (2013). Fighting blindness with microelectronics. *Sci. Transl. Med.* 5:210s16. doi: 10.1126/scitranslmed.3007399

Conflict of Interest Statement: JG provided consulting services for Alpha Omega Co. USA, Inc. and author FH was employed by the company FHC, Inc.

The remaining authors declare that the research was conducted in the absence of any commercial or financial relationships that could be construed as a potential conflict of interest.

Copyright © 2018 Golestanirad, Gale, Manzoor, Park, Glat, Haer, Kaltenbach and Bonmassar. This is an open-access article distributed under the terms of the Creative Commons Attribution License (CC BY). The use, distribution or reproduction in other forums is permitted, provided the original author(s) and the copyright owner(s) are credited and that the original publication in this journal is cited, in accordance with accepted academic practice. No use, distribution or reproduction is permitted which does not comply with these terms.